

## Self-Exploding Lipid-Coated Microgels

Bruno G. De Geest,<sup>†</sup> Barbara G. Stubbe,<sup>†,‡</sup> Alain M. Jonas,<sup>‡</sup> Tinneke Van Thienen,<sup>†</sup> Wouter L. J. Hinrichs,<sup>†</sup> Joseph Demeester,<sup>†</sup> and Stefaan C. De Smedt<sup>\*,†</sup>

Laboratory of General Biochemistry and Physical Pharmacy, Department of Pharmaceutics, Ghent University, Harelbekestraat 72, 9000 Ghent, Belgium, and Unité de Physique et de Chimie des hauts Polymères, Université catholique de Louvain, Croix du Sud, 1-B-1348 Louvain-la-Neuve, Belgium

Received September 29, 2005; Revised Manuscript Received October 26, 2005

Self-exploding microparticles show potential for advanced delivery of certain therapeutics. This study evaluates (1) whether degrading biodegradable dextran hydroxyethyl methacrylate (dex-HEMA) microgels can be coated by a lipid membrane and (2) whether the surrounding membrane can be ruptured by the increasing swelling pressure of the degrading microgel. We found that adsorption of charged liposomes to oppositely charged dex-HEMA microgels provides efficient coating of the microgels, whereby microparticles with a “core–shell” structure were clearly obtained. Especially, we could confirm experimentally that the swelling pressure increase of degrading dex-HEMA microgels can destroy the lipid membrane surrounding the microgels.

### Introduction

Thanks to recent progress in biotechnology and medicine an increasing amount of macromolecular therapeutics (such as proteins and DNA) has become available. As these drugs have to be protected from threatening environments during administration, a lot of scientific effort has been focused on developing appropriate matrixes. Due to their high biocompatibility and tunable properties, hydrogel matrixes are an attractive method to encapsulate such drugs. Our research group is focusing on “exploding microgels” for pulsed drug delivery.<sup>1</sup> We envision micrometer-sized (bio)degradable gel particles surrounded by a membrane that is permeable to water but impermeable to both the entrapped drugs and the degradation products of the gel. As the microgel degrades its swelling pressure increases.<sup>2,3</sup> At a critical value of the swelling pressure we foresee that the membrane will rupture and the entrapped drugs will be released.

Clearly, to realize this concept, one requires a (water permeable) coating surrounding the microgels. Technology that allows coating the surface of hydrogels is very attractive for numerous applications in biomedicine and pharmacy, e.g., for tailoring the hydrophilicity or permeability. However, a general method for the coating of hydrogel surfaces does not yet exist. Obviously, coating microgels demands additional requirements when compared to coating planar supports, a main issue being that the microgels need to remain colloidally stable. Some strategies have been developed to coat microgels with lipids. Kiser et al.<sup>4,5</sup> centrifuged drug-loaded microgels into a lipid film deposited on a glass vial. Several groups modified the hydrogel surface by inserting lipid anchors at the microgel surface, which promote the self-assembly of lipid membranes.<sup>6–9</sup> Although attractive, these methods do show some limitations. For example, when we coated dextran-based microgels by the method of Kiser et al. we observed that only a marginal part of the microgels became lipid coated. Also, the grafting of fatty acid chains on

the microgel's surface, requiring the use of organic solvents, may be hazardous to many biotechnological drugs.

The aim of this paper is twofold. In the first part we aim to demonstrate how dextran hydroxyethyl methacrylate (dex-HEMA) microgels can be coated with lipids, using electrostatic interactions as a driving force. In the second part we aim to show that the increase in swelling pressure, due to the degradation of the dex-HEMA microgels, can rupture the surrounding lipid membrane.

### Materials and Methods

**Materials.** Sulfuric acid (98%), hydrogen peroxide (H<sub>2</sub>O<sub>2</sub>) (30%), and potassium persulfate (KPS) were purchased from Merck VWR. *N,N,N',N'*-Tetramethylethylenediamine (TEMED), methacrylic acid (MAA), dimethyl aminoethyl methacrylate (DMAEMA), chitosan (CHIT; low molecular weight), sodium poly(styrenesulfonate) (PSS, 70 kDa), poly(allylamine hydrochloride) (PAH, 70 kDa), and poly(vinyl alcohol) (PVA, 70 kDa) were obtained from Aldrich. Dextran (19 kDa) and dextran sulfate (DEXS, 500 kDa) were obtained from Fluka. Tetramethyl rhodamine isothiocyanate-dextran (TRITC-dextran, 158 kDa) and fluorescein isothiocyanate-polyallylamine hydrochloride (FITC-PAH, 70 kDa) were purchased from Sigma. The lipids SOPC (stearyl oleoyl phosphatidylcholine), DOPE (dioleoyl glycerol phosphoethanolamine), DOPA (dioleoyl glycerol phosphate), and DOTAP (dioleoyl trimethylammoniumpropane) were obtained from Avanti Polar Lipids. BODIPY was obtained from Molecular Probes. Poly(lactic-co-glycolic) acid (PLGA; 5050 DL 4A) was obtained from Alkermes. One-side-polished 475- $\mu$ m thick silicon wafers were obtained from ACM (Applications Couches Minces, France) with (100) orientation. Table 1 gives an overview of the abbreviations of the polymers and lipids used in this paper.

**Synthesis of Dex-HEMA and Dex-MA.** Dextran-hydroxyethyl methacrylate (dex-HEMA; Figure 1A) and dextran-methacrylate (dex-MA; Figure 1B) were prepared and characterized according to a method described previously.<sup>10</sup> Dextran with a number average molecular weight of 19 kDa was used. The degree of substitution (DS, the number of HEMA groups per 100 glucopyranose residues of dextran) was determined by proton nuclear resonance spectroscopy (<sup>1</sup>H NMR) in D<sub>2</sub>O with a Gemini 300 spectrometer (Varian). The DS of the dex-HEMA and dex-MA used in this study was, respectively, 2.5 and 5.

\* Corresponding author. Phone: 0032-(0)9 264 80 76. Fax: 0032-(0)9 264 81 89. E-mail: Stefaan.Desmedt@ugent.be.

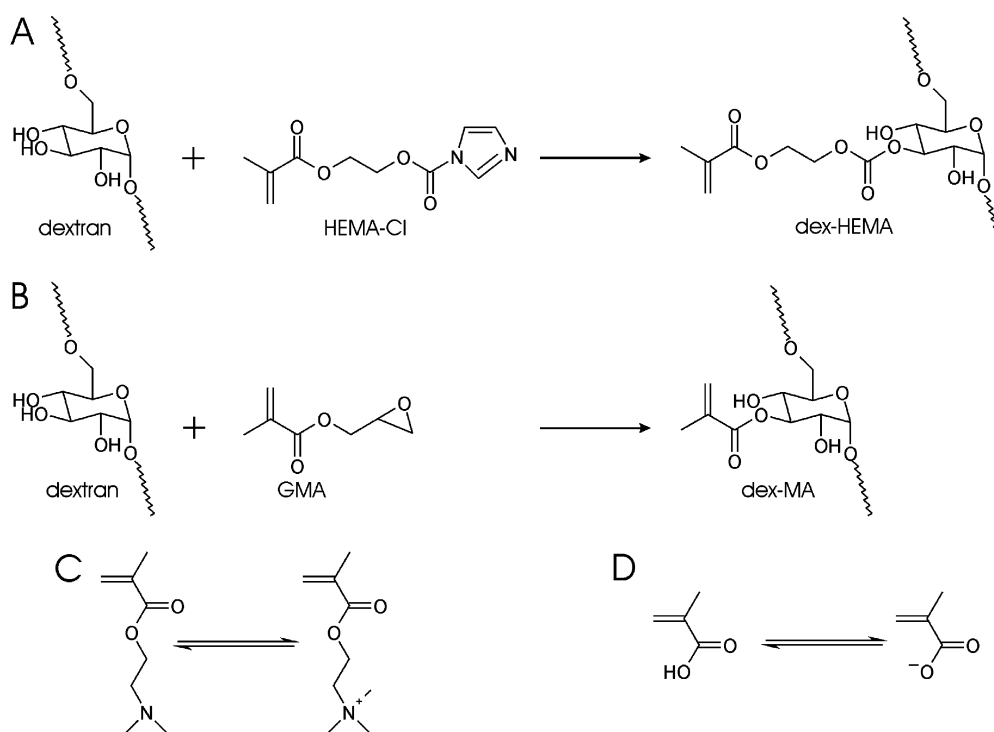
<sup>†</sup> Ghent University.

<sup>‡</sup> Université catholique de Louvain.

<sup>#</sup> This author has equally contributed as first author.

**Table 1.** List of Abbreviations of the Polymers and Lipids Used in This Study

abbreviation	full term	net charge <sup>a</sup>
dex-HEMA	dextran-hydroxyethyl methacrylate	0
dex-MA	dextran-methacrylate	0
dex-HEMA-MAA	dextran-hydroxyethyl methacrylate- <i>co</i> -methacrylic acid	–
dex-HEMA-DMA EMA	dextran-hydroxyethyl methacrylate- <i>co</i> -dimethyl aminoethyl methacrylate	+
dex-MA-MAA	dextran-methacrylate- <i>co</i> -methacrylic acid	–
PLGA	poly(lactic- <i>co</i> -glycolic acid)	–
PAH	poly(allylamine hydrochloride)	+
PSS	poly(styrene sulfonate)	–
CHIT	chitosan	+
DEXS	dextran sulfate	–
SOPC	stearoyl oleoyl phosphatidylcholine	0
DOPA	dioleoyl glycerol phosphate	–
DOTAP	dioleoyl trimethylammoniumpropane	+
DOPE	dioleoyl glycerol phosphoethanolamine	0

<sup>a</sup> Under physiological conditions.**Figure 1.** Synthesis of dex-HEMA (A) and dex-MA (B). The chemical structure of DMAEMA is shown in (C) and that of MAA is shown in (D).

**Preparation of Dex-HEMA Microgels.** Dex-HEMA microgels were prepared according to Stenekes et al.<sup>11</sup> In detail, deoxygenated aqueous solutions of dex-HEMA (25% w/w solution) and poly(ethylene glycol) (PEG; 24% w/w solution; 20 kDa) were prepared. The dex-HEMA and PEG solutions were vigorously mixed with a vortex for 1 min under a nitrogen atmosphere to obtain a water-in-water emulsion. A PEG/dex-HEMA ratio of 19 (v/v) was used; the total volume amounted to 5 mL. The resulting emulsion was allowed to stabilize for 10–15 min. Subsequently TEMED (100  $\mu$ L pH neutralized with 4 N HCl) and KPS (180  $\mu$ L, 41 mM) were added to cross-link the dex-HEMA. After gentle mixing, the emulsion was incubated without stirring for 30 min at 40 °C yielding microgels with an estimated water content of approximately 60% (w/w).<sup>12</sup> Three washing and centrifugation steps with 50 mL of Milli-Q water removed the residual KPS and TEMED. The remaining pellet was suspended in 5 mL of Milli-Q water.

To prepare negatively and positively charged dex-HEMA microgels,<sup>13</sup> respectively, methacrylic acid (MAA; 25  $\mu$ L) or dimethyl aminoethyl methacrylate (DMAEMA; 35  $\mu$ L) was added to the mixture just before vortexing the dextran and PEG solutions as described in

the paragraph above. In this paper “dex-HEMA-MAA microgels” and “dex-HEMA-DMAEMA microgels” refer to negatively charged and positively charged microgels, respectively.

Dex-MA microgels were fabricated in an identical way as dex-HEMA microgels.

**Preparation of PLGA Microparticles.** An amount of 100 mg of PLGA was dissolved in 10 mL of dichloromethane. An amount of 100 mg of PVA was dissolved in 100 mL of water. Both solutions were mixed by vortexing for 1 min yielding an emulsion of dichloromethane in water. A volume of 50 mL of water was added, and the emulsion was stirred for 3 h at 40 °C to evaporate the dichloromethane. The resulting PLGA microparticles were centrifuged and washed twice with Milli-Q water. Afterward they were stored at 4 °C.

**Lipid Coating of Dex-HEMA Microgels.** The lipid vesicles were prepared as follows. The lipids were first dissolved in chloroform (2 mg/mL). Subsequently, the chloroform was evaporated yielding a lipid film on a glass vial. To obtain lipid vesicles (liposomes), water was added up to a final lipid concentration of 1 mg/mL, and the mixture was sonicated (Branson 32, Branson Ultrasonics, 150 W) for 5 min.

To reduce the size of the liposomes, the liposomes were extruded through a carbonate membrane with a pore size of 100 nm.

The (charged) liposomes (500  $\mu\text{L}$ ) were mixed with a suspension (200  $\mu\text{L}$ ) of (oppositely charged) microgels and shaken for 20 min to allow adsorption of the lipid vesicles to the surface of the microgels. Then the samples were centrifuged for 3 min at 500g, and the supernatants were removed. The centrifugation and resuspension procedure was repeated three times. Finally, the microgels were redispersed in 500  $\mu\text{L}$  of Milli-Q water and stored at 4 °C.

**Lipid Coating of PLGA Microparticles.** The PLGA microparticles were first “precoated” with three polyelectrolyte bilayers by alternating immersion in aqueous solutions of dextran sulfate (2 mg/mL) and chitosan (1 mg/mL) in the presence of 0.5 M NaCl. The polyelectrolytes were allowed to adsorb for 15 min, under continuous gentle shaking. The dispersion was then centrifuged, and the supernatant was removed. Afterward, the microparticles were redispersed in Milli-Q water to wash away the nonadsorbed polyelectrolytes. This washing was repeated twice before the second polyelectrolyte solution was added. The process was repeated until three bilayers were deposited.

In a final step, the precoated PLGA particles were lipid coated, following the same procedure as for the lipid coating of microgels.

**Degradation Experiments.** To visualize the degradation behavior of the (lipid-coated) microgels a 10  $\mu\text{L}$  drop of microgel suspension was put at room temperature on a coverslip under the confocal microscope. To accelerate the degradation rate of the (lipid-coated) microgels, 10  $\mu\text{L}$  of a 1 M NaOH solution was added to the drop of microgel suspension, and the behavior of the microgels was followed under the confocal microscope.

**Confocal Laser Scanning Microscopy.** Confocal micrographs of the lipid-coated microgels and PLGA microparticles were taken with a MRC1024 Bio-Rad confocal laser scanning microscope (CLSM) equipped with a krypton–argon laser (Biorad, Cheshire, U.K.). An inverted microscope (Eclipse TE300D, Nikon, Japan) was used which was equipped with a water immersion objective lens (Plan Apo 60 $\times$ , NA 1.2, collar rim correction, Nikon, Japan). Dex-HEMA microgels were made fluorescent by adding 1 mg of TRITC-labeled dextrans to the dex-HEMA/PEG mixture before the cross-linking.

**Electrophoretic Mobility.** The electrophoretic mobility of the layer-by-layer (LbL)-coated microgels was measured using a Malvern Zetasizer 2000 (Malvern Instruments, Worcestershire, U.K.). The  $\zeta$ -potential was calculated from the electrophoretic mobility ( $\mu$ ) using the Smoluchowski relation:

$$\zeta = \mu\eta/\epsilon$$

where  $\eta$  and  $\epsilon$  are the viscosity and permittivity of the solvent, respectively.

**Scanning Electron Microscopy (SEM).** Samples for scanning electron microscopy (SEM) imaging were prepared by drying under vacuum followed by sputtering with chrome. SEM images were recorded using a Gemini Leo 982, operating at an accelerating voltage of 1 kV.

**Lipid Coating of Silicon Wafers.** One-side-polished 475- $\mu\text{m}$  thick silicon wafers were cut into rectangles (2  $\times$  3  $\text{cm}^2$ ). The wafers were cleaned for 20 min in freshly prepared piranha solutions ( $\text{H}_2\text{O}_2$  (30%)/ $\text{H}_2\text{SO}_4$  (98%) 1:1 v/v (*caution: piranha solutions react violently with organic materials and should not be stored in closed containers*), then abundantly rinsed with Milli-Q water. Wafers were dried by spinning with a spin coater.

Prior to adding the lipid coating to the silicon wafers, polyelectrolyte multilayers were first deposited by alternating dipping of the silicon wafers in aqueous solutions of dextran sulfate (2 mg/mL) and chitosan (1 mg/mL) in the presence of 0.5 M NaCl for 5 min. Three rinsing steps in Milli-Q water and one drying step were applied between each adsorption step. This process was repeated three times. Thereafter, the SOPC/DOTAP (9:1) lipid layer was deposited by dipping the polyelectrolyte-coated silicon wafer in a lipid vesicle dispersion prepared as described above.

**Ellipsometry.** The thickness of the film deposited on the silicon wafers was determined in air with a null ellipsometer (Multiskop from Optrel, Berlin, Germany) at a fixed incident angle of 70° and a fixed wavelength of 5320 Å. A refractive index of 1.48 was assumed to determine the film thickness.

**X-ray Reflectometry (XRR).** The experimental setup consists of a Siemens D5000 2-circles goniometer of 30-cm radius and 0.002° positioning accuracy. X-rays of 1.5418 Å wavelength (Cu K $\alpha$ ) were obtained from a Siemens rotating anode operated at 40 kV and 300 mA, fitted with a graphite secondary monochromator and a scintillation counter. The beam was defined by a 40- $\mu\text{m}$  wide slit placed at 17.5 cm from the focal point. Parastatic scattering was decreased by a 200- $\mu\text{m}$  wide slit placed after the 40- $\mu\text{m}$  slit. The sample was placed at the center of the goniometer with an automated procedure, using a vertical stage of 1- $\mu\text{m}$  resolution. The intensity was scaled to unit incident intensity and then corrected for spill-over at very low angles of incidence. Data are reported as a function of  $k_{z0}$ , the vertical component of the wave vector of the incident photons in a vacuum.

XRR data were analyzed in two ways. First a Patterson function was computed from the data as described elsewhere,<sup>14</sup> and the average thickness of the coating was obtained from the position of the subsidiary correlation peak in this function. Second, a model of electron density was fitted to the data. The electron density profile was discretized as a succession of flat slabs of width  $\Delta = 0.5$  nm, approximately corresponding to the resolution of the experiments defined by  $k_{z0,\text{max}}$ , the maximum value of  $k_{z0}$  for which the signal is not yet dominated by the background ( $\Delta = \pi/(2k_{z0,\text{max}})$ ). The number of slabs required was initially selected from the known thickness of the coating determined by the Patterson function. It was progressively incremented to take into account the width of the interfaces, until the fit was deemed satisfactory as judged from the value of  $\chi^2$  obtained. The fit parameters were the height (electron density) of each slab, a general scaling parameter, and a constant background value. The reflectivity was computed using Paratt's formalism.<sup>15,16</sup> To ease interpretation, the electron density profiles are represented by dots placed at the centers of each slab; cubic spline interpolation of these profiles was used to draw a smooth line through the dots.

## Results and Discussion

Dex-HEMA (Figure 1A) and dex-MA (Figure 1B) were synthesized according to van Dijk-Wolthuis et al.<sup>10</sup> by grafting dextran with carbonyl imidazole activated HEMA (HEMA-CI) and glycidyl methacrylate (GMA), respectively. Microgels were synthesized using an all-aqueous water-in-water emulsion technique based on the immiscibility of a dex-(HE)/MA and a poly(ethylene glycol) (PEG) phase.<sup>17</sup> In a first approach we tried to coat the dex-HEMA microgels by centrifuging the microgels into a lipid film at the bottom of the test tube, following the procedure reported by Kiser et al.<sup>4,5</sup> However, in this way only a low percentage of the dex-HEMA microgels became lipid coated. Looking further for a more efficient way to coat the dex-HEMA microgels with a lipid membrane we thought to make charged microgels and coat them with oppositely charged lipids, using electrostatic attractions as the driving force. Addition of DMAEMA ( $\text{pK}_a = 8.3$ ; Figure 1C) and respectively MAA ( $\text{pK}_a = 4.5$ ; Figure 1D) during synthesis of the dex-HEMA microgels allowed us to obtain, respectively, positively and negatively charged dex-HEMA microgels, as evidenced from  $\zeta$ -potential measurements (Figure 2A).

In this study SOPC/DOPA, SOPC/DOTAP, and DOPE/DOTAP (all with a molar ratio of 9:1) liposomes were used. SOPC and DOPE are both neutral lipids, while DOPA and DOTAP are, respectively, negatively and positively charged. For the formation of unilamellar liposomes it is important that the temperature at which the experiments are performed is above



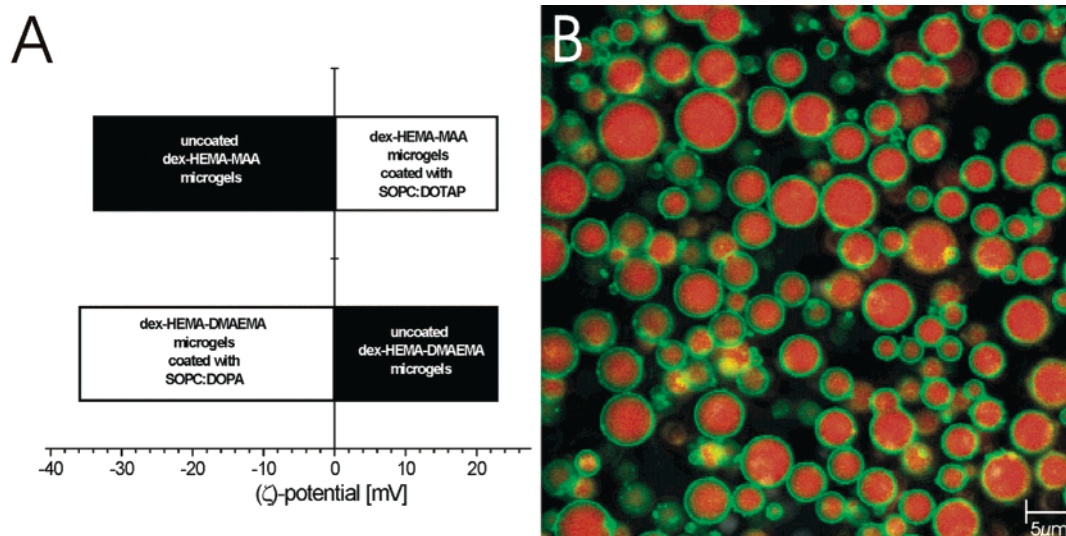


**Figure 2.** (A)  $\zeta$ -Potential of dex-HEMA-MAA and dex-HEMA-DMAEMA microgels, respectively, before and after coating with oppositely charged lipid vesicles. (B) CLSM images of dex-HEMA-DMAEMA microgels coated with SOPC/DOPA; the microgels themselves are fluorescently labeled with TRITC-dextrans, while the lipids are labeled with BODIPY.

the phase transition temperature of the lipids. For all the lipids used in this study the phase transition temperature is below or equal to 0 °C,<sup>18</sup> allowing one to perform the experiments at room temperature. The combination of charged lipids with neutral lipids is necessary to avoid too much repulsion within the bilayers and thus allow stable vesicles to form. CLSM clearly showed that upon exposure to the SOPC/DOPA lipid vesicles all the dex-HEMA-DMAEMA microgels became lipid coated (Figure 2B). Microparticles with a core-shell structure were obtained with lipids only at the surface of the microgels and not in the interior. We assume that the liposomes electrostatically interact with the charges at the microgel surface. Once the surface of a microgel is covered, the lipid vesicles probably spread open and form a lipid layer. Spreading of liposomes upon adsorption on a solid substrate has been observed by several other groups.<sup>19–22</sup> Recently Mornet et al.<sup>22</sup> reported on the coating of silica particles with a lipid bilayer. They observed with cryo electron microscopy that the lipid bilayer faithfully follows the contour of the solid support. Also they reported that to achieve spreading and fusing of the liposomes a ratio of neutral to charged lipids of at least 3:1 was required. Liposomes with a higher net charge did not tend to spread, possibly due to electrostatic repulsion; this contributes to our choice of using liposomes with a ratio of uncharged lipids to charged lipids of 9:1.

Besides CSLM, electrophoretic mobility measurements also proved that the dex-HEMA microgels became lipid coated. Figure 2A shows that the  $\zeta$ -potential of the microgels indeed inverted upon exposure to oppositely charged lipid vesicles. The morphology of both the lipid-coated and uncoated microgels was further characterized by scanning electron microscopy (SEM). Figure 3, parts A and B reveal that the surface of the uncoated microgels is smoother compared to the surface of the coated microgels. The observation of a rather rough surface of the lipid-coated microgels can most likely be attributed to the differential drying of the microgel core and the lipid coating.

To evaluate to what extent this way of lipid coating is broadly applicable on microparticles we performed experiments on neutral dex-HEMA microgels (Figure 4, parts A and B) and PLGA particles (Figure 4C). Both types of particles could be successfully coated with lipids if a polyelectrolyte film was first deposited onto the surface of the particles to introduce charges

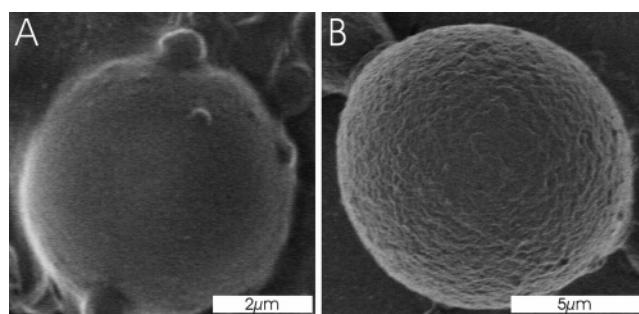


**Figure 3.** (A) SEM image of uncoated dex-HEMA-DMAEMA microgels. (B) SEM image of SOPC/DOPA-coated dex-HEMA-DMAEMA microgels.

at the surface. Using the layer-by-layer (LbL) technique, as developed on colloidal particles by Sukhorukov and co-workers,<sup>23,24</sup> we deposited two polyelectrolyte bilayers (using poly(styrenesulfonate) (PSS) and poly(allylamine) hydrochloride (PAH)) and one monolayer of PSS (denoted as (PSS/PAH)<sub>2</sub>PSS) on the neutral dex-HEMA microgels. On the PLGA particles a precursor film consisting of dextran sulfate (DEXS) and chitosan (CHIT) (denoted as (DEXS/CHIT)<sub>2</sub>DEXS) was applied. This “precoating step” with polyelectrolytes was performed by submerging the microgels for 15 min in a 2 mg/mL polyelectrolyte solution containing 0.5 M NaCl, followed by two rinsing steps with pure water. The precoating step with polyelectrolytes was necessary, most likely to create a sufficient surface charge in order to electrostatically attract the liposomes, as a lipid coating could not be applied on PLGA particles or on neutral dex-HEMA microgels without a polyelectrolyte multilayer at their surface. Similarly it was not possible to coat microgels with only neutral charged lipids or with lipids bearing an equal charge as the microgels, indicating that electrostatic interactions play a major role in the lipid-coating process we describe in this paper.

Although the deposition of a lipid layer on the dex-HEMA microgels was evidenced we did not know whether one lipid bilayer or multiple lipid bilayers were formed. XRR is ideally suited to investigate the structure of ordered films.<sup>14</sup> As XRR should be performed in the dry state and on flat substrates it cannot be applied to microgels. To obtain some more insight into the deposition of charged lipids onto an oppositely charged

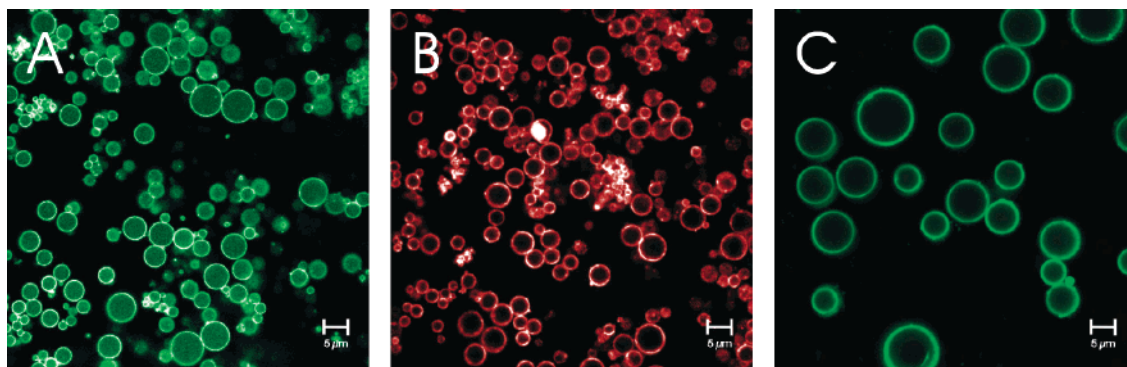


**Figure 4.** (A) Green and (B) red fluorescence image of neutral dex-HEMA microgels first precoated with  $(\text{PSS}/\text{PAH})_2\text{PSS}$  and then coated with DOPE/DOTAP; PAH was FITC labeled, and DOPE was rhodamine labeled. (C) PLGA microspheres first precoated with  $(\text{CHIT}/\text{DEXS})_3$  and then coated with DOPE/DOTAP. The lipids were labeled with BODIPY.

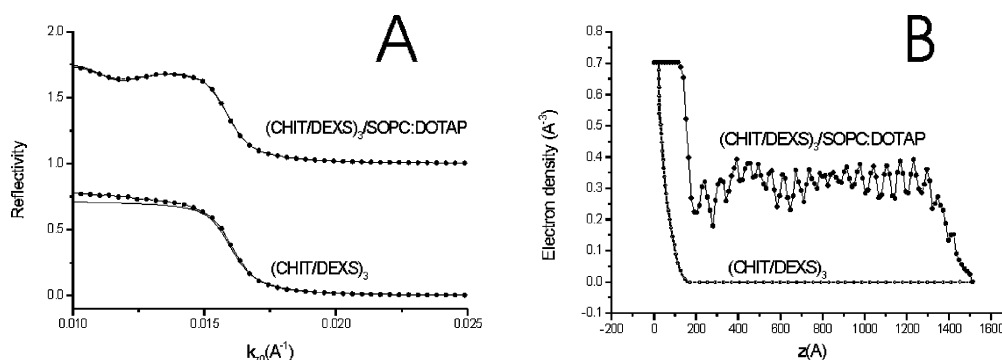


**Figure 5.** (A) X-ray reflectivity of silicon wafers coated with, respectively,  $(\text{CHIT}/\text{DEXS})_3$  and  $(\text{CHIT}/\text{DEXS})_3/\text{SOPC}:\text{DOTAP}$ . Circles are experimental data. Lines are fits using the electron density profiles shown in part B. For clarity, the curves have been displaced vertically. The term  $k_{z0}$  is the vertical component of the wave vector of the incident photons in vacuum. (B) Corresponding electron density profiles. Circles correspond to computed densities, and continuous lines were obtained by cubic spline interpolation.

surface we exposed liposomes to a silicon wafer onto which three bilayers of CHIT/DEXS were deposited. However this surface probably differs largely from that of the microgel's surface, it can serve as a model surface and will aid in understanding the lipid-coating process. Figure 5 shows the X-ray reflectograms and the corresponding electron density profiles of  $(\text{CHIT}/\text{DEXS})_3$  and  $(\text{CHIT}/\text{DEXS})_3/\text{SOPC}:\text{DOTAP}$ -coated silicon wafers. From the number of Bragg peaks we estimated<sup>13</sup> that the lipid coating obtained on the silicon wafers consists of approximately 20 lipid bilayers, leading to a total thickness of 120 nm. As verification we measured the film thickness by ellipsometry and found a thickness of 119 nm which agrees with the XRR data. The absence of Kiessig fringes points toward a high roughness of the coating, most probably because the surface consists of steps of discrete height (integral multiples of the period), giving a cityscape profile to the surface. Clearly, we cannot literally extend the observations made on the (flat) lipid-coated silicon surface to the (spherical) lipid-coated microgel surface. However, these observations allow speculating that the dex-HEMA microgels are probably covered with multiple lipid bilayers. From the XRR measurements it is most likely that upon adsorption the liposomes indeed fuse and spread resulting in a coating consisting of multiple lipid bilayers. In case the lipid coating would consist of intact nonfused liposomes it would be probably impossible to detect the 20 Bragg peaks, the width of each peak corresponding with a bilayer thickness of 6 nm which agrees well with literature data on the thickness of lipid bilayers.<sup>22</sup>

As outlined in the Introduction, the second aim of this work was to evaluate whether the swelling pressure of the degrading dex-HEMA microgels can rupture the surrounding lipid membrane. The degradation of dex-HEMA, by hydrolysis of the

carbonate esters (indicated in Figure 1) that connect the methacrylate groups with the dextran backbone, results in high molecular weight dextran chains (19 kDa) and HEMA oligomers.<sup>10</sup> By hydrolysis of the carbonate esters, the cross-links, which connect the dextran chains in the microgels, cleave. This lowers the elasticity of the microgels which, in turn, increases the swelling pressure of the dex-HEMA microgels.<sup>2,3</sup> In previous work, our group characterized how the swelling pressure of degrading dex-HEMA gels increases during degradation and showed that, when the gel becomes totally degraded, the swelling pressure at the end of the degradation equals the osmotic pressure of the obtained dextran solution. The swelling pressure of the completely degraded dex-HEMA hydrogels used in this study was previously determined to be around 150 kPa.<sup>3</sup> As lipids are known to have a limited permeability,<sup>25</sup> we expected that the degradation products of the dex-HEMA microgels would not diffuse through the lipid membrane before the rupturing of the membrane. To accelerate the degradation of the lipid-coated dex-HEMA microgels, which ranges at neutral pH from days to weeks depending on the composition of the gel,<sup>17</sup> we added a sodium hydroxide solution (NaOH; 1 M) to the dispersion of lipid-coated dex-HEMA microgels. Under these alkaline conditions hydrolysis of the dex-HEMA microgels occurs within minutes. Figure 6 shows CLSM snapshots, taken every 15 s, of the process. Initially, during the first 75 s, the lipid membrane inflates and stretches, due to the increasing swelling pressure of the degrading dex-HEMA microgels. Finally, in the time interval between 75 and 90 s, this swelling pressure causes the rupture of the lipid membrane (as Supporting Information a movie is provided showing the explosion of a larger amount of lipid-coated microgels, showing that all particles behaved in a similar way during degradation)

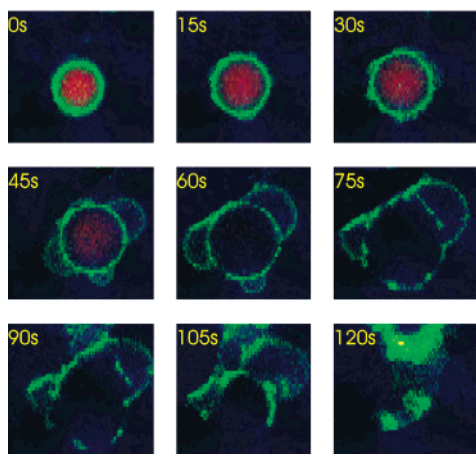


**Figure 6.** CLSM snapshots of degrading dex-HEMA-MAA microgels, coated with SOPC/DOTAP. The first image (0 s) is obtained immediately after the addition of sodium hydroxide to the microgels. The subsequent images are taken every 15 s. The lipids are green labeled using BODIPY, while the microgels are red labeled using TRITC-dextran. Note that the fade out of the red color is not due to bleaching or leakage of the TRITC-dextran from the microgels but to the pH-dependent fluorescence of TRITC. After explosion of the microgels (120 s) only remnants of the lipids can be observed.

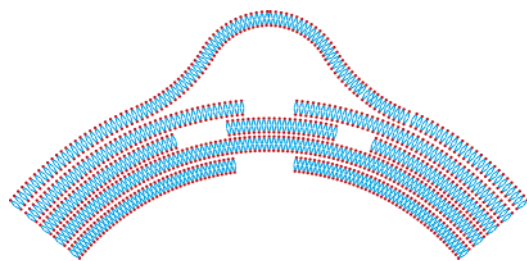


**Figure 7.** "Parachute" formation in the top bilayer during degradation of the dex-HEMA microgels. Discontinuities within a single lipid bilayer may allow the swelling pressure to inflate the top layer before complete rupturing of the lipid membrane.

leading to a collapsed lipid membrane as is clearly shown in the image after 120 s. During the "stretch phase" of the lipid membrane we also observed the formation of "parachutes" on the microgels preceding the complete explosion of the lipid membrane. The formation of these parachutes supports the hypothesis that the lipid film consists of multiple lipid bilayers which elongate, creating additional surface area, when subjected to the swelling pressure of the degrading microgel. As schematically outlined in Figure 7, at certain locations the lipid membrane may be weaker than at other locations due to discontinuities within single lipid bilayers. While the swelling pressure of the degrading microgel inflates the whole lipid membrane, at these weaker places in the membrane the increasing swelling pressure locally inflates the lipid membrane resulting in the formation of parachutes.

As the microgels immediately began to degrade upon exposure to NaOH it seems that the hydroxyl ions are able to diffuse through the lipid coating. On the other hand, the lipid coating appears to be impermeable to the degradation products of the microgels: they seem to remain in the lipid-coated particles as an increase in osmotic pressure occurs which finally results in the rupturing of the lipid membrane. Several groups<sup>18,26,27</sup> have observed that *supported* lipid bilayers are permeable to small molecules, whereas the corresponding liposomes seem impermeable to the same molecules. For example Ng et al. reported on lipid membranes supported on hydrogel beads which were impermeable to dextrans with a

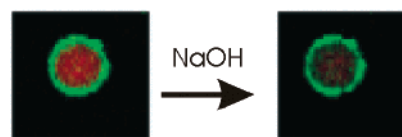


**Figure 8.** Lipid (SOPC/DOTAP)-coated dex-MA-MAA microgels before and after the addition of sodium hydroxide. The lipid membrane remains intact. Note that the same fading of the red fluorescence occurs as observed in Figure 6, due to the pH-dependent fluorescence of TRITC.

molecular weight ranging from 1.5 to 3 kDa, whereas the membrane appeared to be permeable to calcium ions.<sup>27</sup> This permeability was attributed to the presence of small nanoscopic defects within the lipid bilayers allowing the diffusion of small molecules. Most likely a similar phenomenon occurs in case of lipid coating of dex-HEMA microgels.

In the degradation experiment presented in Figure 6 the lipid-coated microgels were immersed in an alkaline solution. One could, however, wonder whether the alkaline medium did not damage the lipid coating, leading to a desorption from the microgel surface. To elucidate this we prepared lipid-coated (SOPC/DOTAP (9:1)) dextran-methacrylate (dex-MA; Figure 1B) hydrogels containing MAA. While dex-HEMA hydrogels degrade through hydrolysis, dex-MA gels do not as no carbonate esters are present in the cross-links.<sup>10</sup> When 1 M sodium hydroxide was added to uncoated dex-MA-MAA microgels they remained intact (data not shown). A similar behavior was observed when lipid-coated dex-MA-MAA microgels were brought into contact with sodium hydroxide: the lipid film remained intact (lipid-coated dex-MA-MAA microgels were exposed to the NaOH for at least 1 h), parachute formation did not occur, and the lipid coating did not desorb (Figure 8), all indicating that addition of NaOH does not influence the lipid bilayer itself. This allowed us to conclude that the rupture of the lipid membrane surrounding the dex-HEMA microgels upon addition of NaOH (Figure 6) is indeed attributed to the increase in swelling pressure of the degrading dex-HEMA core and not to NaOH-induced weakening of the lipid membrane.

In the above sections we have shown that the swelling pressure of the degrading microgels can result in a rupturing of the surrounding lipid membranes. It can be argued that we were not able to deposit only a single lipid bilayer on the surface of the dex-HEMA microgels. However, multiple bilayers surrounding the microgels may provide us with a more robust system being more versatile for real applications. The use of 1 M NaOH to trigger the explosion of the lipid coating is clearly not a stimulus which can be provided by the human body in vivo. However, the only aim of adding NaOH was to accelerate the degradation of the lipid-coated microgels in order to visualize their behavior in a reasonable time frame using confocal microscopy. To confirm that the explosion of the lipid coating also occurs at physiological conditions, the lipid-coated dex-HEMA-DMAEMA microgels were incubated at 37 °C in phosphate-buffered saline; after 7 days lipid-coated microgels could not be detected anymore indicating the degradation of the microgels and rupturing of the lipid coating.

## Conclusions

In this paper we have demonstrated a new method for the lipid coating of microgels based on electrostatic interactions between the microgel's charged surface and oppositely charged lipid vesicles. We have also demonstrated that this way of lipid coating is also applicable on noncharged microgels as well as



PLGA particles, given that charges are introduced at their surface by applying a polyelectrolyte multilayer by the LbL approach. The lipid coating thus obtained very likely consists of multiple lipid bilayers and shows certain defects. We showed that the increase in swelling pressure, which occurs in degrading dex-HEMA microgels, did indeed rupture the surrounding lipid membrane.

The prepared microgels may be promising for pulsed drug delivery applications. As the composition (i.e., cross-link density) of the dex-HEMA microgels governs their degradation rate, and therefore how their swelling pressure increases,<sup>2,3</sup> it may allow one to tailor the time of explosion of the lipid-coated microgels by varying their composition. Using this concept one may be able to design a drug formulation which delivers the drug in a number of pulses after a single injection: a simultaneous injection of, e.g., three populations of lipid-coated dex-HEMA microgels, each population exploding at a well-defined time after injection, may result in three drug pulses from a single injection. This clearly differs from other types of degradable microparticles that release the encapsulated drugs in a, more or less, constant rate.<sup>28–30</sup>

While others<sup>4,5</sup> have reported on lipid-coated microgels in which the lipid membrane is ruptured by an external trigger (e.g., electric field), the lipids surrounding the microgels presented in this paper are ruptured by an internal trigger, namely at the moment the swelling pressure of the dex-HEMA reaches a critical value. To demonstrate the concept we used NaOH to trigger the rupturing of the coating. However, as the degradation of the microgels also occurs at physiological conditions the lipid-coated microgels presented in this study can be termed as “self-exploding microgels”. Our future research will focus on the release of macromolecules from such self-exploding microgels.

**Acknowledgment.** Wim Hennink, Mies van Steenberghe, Sophie Van Tomme, and Laura Delaporte are gratefully thanked for valuable discussions. We acknowledge Etienne Ferain for taking SEM images, and Ghent University (BOF) is acknowledged for a scholarship (B.G.D.G.) and instrumentation credits.

**Supporting Information Available.** Movie showing the explosion of lipid-coated microgels. This material is available free of charge via the Internet at <http://pubs.acs.org>.

## References and Notes

- (1) De Geest, B. G.; Dejugnat, C.; Sukhorukov, G. B.; Braeckmans, K.; De Smedt, S. C.; Demeester, J. *Adv. Mater.* **2005**, *17*, 2357–2361.
- (2) Stubbe, B. G.; Braeckmans, K.; Horkay, F.; Hennink, W. E.; De Smedt, S. C.; Demeester, J. *Macromolecules* **2002**, *357*, 2501–2505.
- (3) Stubbe, B. G.; Horkay, F.; Amsden, B.; Hennink, W. E.; De Smedt, S. C.; Demeester, J. *Biomacromolecules* **2003**, *4*, 691–695.
- (4) Kiser, P. F.; Wilson, G.; Needham, D. *Nature* **1998**, *394*, 459–62.
- (5) Kiser, P. F.; Wilson, G.; Needham, D. *J. Controlled Release* **2000**, *68*, 9–22.
- (6) Major, M.; Prieur, E.; Tocanne, J. F.; Betbeder, D.; Sautereau, A. *M. Biochim. Biophys. Acta: Biomembranes* **1997**, *1327*, 32–40.
- (7) Jin, T.; Pennefather, P.; Lee, P. I. *FEBS Lett.* **1996**, *397*, 70–74.
- (8) Kraft, M. L.; Moore, J. S. *J. Am. Chem. Soc.* **2001**, *123*, 12921–12922.
- (9) Ng, C. C.; Cheng, Y. L.; Pennefather, P. S. *Macromolecules* **2001**, *34*, 5759–5765.
- (10) van Dijk-Wolthuis, W. N. E.; Tsang, S. K. Y.; Kettenes-vanden Bosch, J. J.; Hennink, W. E. *Polymer* **1997**, *38*, 6235–6242.
- (11) Stenekes, R. J. H.; Franssen, O.; van Bommel, E. M. G.; Crommelin, D. J. A.; Hennink, W. E. *Pharm. Res.* **1998**, *15*, 557–561.
- (12) Stenekes, R. J. H.; Hennink, W. E. *Int. J. Pharm.* **1999**, *189*, 131–155.
- (13) Van Tomme, S. R.; van Steenberghe, M. J.; De Smedt, S. C.; van Nostrum, C. F.; Hennink, W. E. *Biomaterials* **2005**, *26*, 2129–35.
- (14) Arys, X.; Laschewsky, A.; Jonas, A. M. *Macromolecules* **2001**, *34*, 3318–3330.
- (15) Parratt, L. G. *Phys. Rev.* **1954**, *95*, 359–69.
- (16) Parratt, L. G. *J. Chem. Phys.* **1956**, *53*, 597.
- (17) Franssen, O.; Hennink, W. E. *Int. J. Pharm.* **1998**, *168*, 1–7.
- (18) As stated by the manufacturer.
- (19) Nollert, P.; Kiefer, H.; Jahnig, F. *Biophys. J.* **1995**, *69*, 1447–1455.
- (20) Moya, S.; Richter, W.; Leporatti, S.; Baumler, H.; Donath, E. *Biomacromolecules* **2003**, *4*, 808–814.
- (21) Troutier, A. L.; Delair, T.; Pichot, C.; Ladaviere, C. *Langmuir* **2005**, *21*, 1305–1313.
- (22) Mornet, S.; Lambert, O.; Duguet, E.; Brison, A. *Nano Lett.* **2005**, *5*, 281–85.
- (23) Sukhorukov, G. B.; Donath, E.; Lichtenfeld, H.; Knippel, E.; Knippel, M.; Budde, A.; Mohwald, H. *Colloids Surf., A* **1998**, *137*, 253–266.
- (24) Moya, S.; Donath, E.; Sukhorukov, G. B.; Auch, M.; Baumler, H.; Lichtenfeld, H.; Mohwald, H. *Macromolecules* **2000**, *33*, 4538–44.
- (25) Olbrich, K.; Rawicz, W.; Needham, D.; Evans, E. *Biophys. J.* **2000**, *79*, 321–27.
- (26) Buck, S.; Pennefather, P. S.; Xue, H. Y.; Grant, J.; Cheng, Y.-L.; Allen, C. J. *Biomacromolecules* **2004**, *5*, 2230–2237.
- (27) Ng, C. C.; Cheng, Y.-L.; Pennefather, P. S. *Biophys. J.* **2004**, *87*, 323–331.
- (28) Hanes, J.; Cleland, J. L.; Langer, R. *Adv. Drug Delivery Rev.* **1997**, *28*, 97–119.
- (29) Langer, R. *Nature* **1998**, *392*, 5–10.
- (30) Zhao, Z.; Wang, J.; Mao, H. Q.; Leong, K. W. *Adv. Drug Delivery Rev.* **2003**, *55*, 483–499.

BM0507296